

# Mapping the spatial distribution of entanglement in optical lattices

Emilio Alba,<sup>1</sup> Géza Tóth,<sup>2,3,4</sup> and Juan José García-Ripoll<sup>1</sup>

<sup>1</sup>*Instituto de Física Fundamental, Consejo Superior de Investigaciones Científicas, Calle Serrano 113b, Madrid E-28006, Spain*

<sup>2</sup>*Department of Theoretical Physics, The University of the Basque Country, P.O. Box 644, E-48080 Bilbao, Spain*

<sup>3</sup>*IKERBASQUE, Basque Foundation for Science, E-48011 Bilbao, Spain*

<sup>4</sup>*Research Institute for Solid State Physics and Optics, Hungarian Academy of Sciences, P.O. Box 49, H-1525 Budapest, Hungary*

(Received 12 July 2010; published 21 December 2010; publisher error corrected 21 January 2011)

In this work we study the entangled states that can be created in bipartite two-dimensional optical lattices loaded with ultracold atoms. We show that, by using only two sets of measurements, it is possible to compute a set of entanglement witness operators distributed over arbitrarily large regions of the lattice, and use these witnesses to produce two-dimensional plots of the entanglement content of these states. We also discuss the influence of noise on the states and on the witnesses, as well as the relation to ongoing experiments.

DOI: [10.1103/PhysRevA.82.062321](https://doi.org/10.1103/PhysRevA.82.062321)

PACS number(s): 03.67.Mn, 03.75.Gg, 42.50.Dv

## I. INTRODUCTION

The quantum engineering of useful many-body states and the characterization of their entanglement properties are two of the most challenging topics in Quantum Information Science, both theoretically and experimentally. In the laboratory, the creation of entangled states has been addressed in two ways. The first one starts from the control of individual quantum systems (e.g., photons [1–4], neutral atoms [5,6] or ions [7,8]), and aims at the creation of ever larger many-body states. The second one consists of taking large numbers of these components (e.g.,  $10^3$ – $10^6$  atoms) and studying collective degrees of freedom [9]. It thus seems that one has to make a compromise between having large entangled states or having a fine-grained knowledge of the properties of the state.

In this work we show that there is an intermediate approach, by which it is possible to gain local information about a very large entangled state. More precisely, we introduce a family of operators that allow for obtaining lower bounds on the fidelity or detecting multipartite entanglement in regions of a two-dimensional (2D) graph state. The entanglement witnesses [10–14] are optimized for setups with ultracold atoms in 2D bipartite lattices, in which one now has access to the state of individual atoms [15,16]. Remarkably, our witnesses only require the simultaneous measurement of all atoms, but with a postprocessing of the measurement statistics they provide a map of the quality and multipartite entanglement of the many-body state.

This paper is structured as follows: In Sec. II we review the experimental techniques available to create graph states in optical lattices. We present observables that characterize the state and act as entanglement witnesses in Sec. III, in which we also face the main difficulties associated with this method. We find that even under decoherence, states that are useful for quantum computation can be found, and we analyze simple observables that bound the fidelity of the state. Finally, in Sec. IV, we perform numerical simulations of a cluster state subject to different noise sources, demonstrating that the entanglement witness is capable of detecting those errors.

## II. EXPERIMENTAL GENERATION OF STABILIZER STATES

The original method for creating graph states with neutral atoms [17] was based on filling state-dependent lattices with

one atomic species and using controlled collisions [18,19]. In contrast, we will develop our ideas by building on the experimental setup from Refs. [16,20], which traps two different species of atoms in two coexisting optical lattices, one of which can be moved. This setup combines a diffraction mask with a powerful microscope objective, which projects two similar triangular lattice patterns on its focal plane. By using two light beams with different frequencies, the experiment may trap lithium and cesium atoms in two independent lattices that can be moved at will along the plane that confines the atoms. As shown in Fig. 1(a), we can contemplate the Cs and Li arrangements as the triangular sublattices of a larger honeycomb lattice in which each Cs atom is surrounded by three Li atoms (and vice versa), and each atom acts as one qubit. Since our lattice is bipartite by construction, entanglement can be created by using a small number of steps, equal to the coordination number of the full lattice. Continuing with this example, one has to move one sublattice three times so that each Cs atom approaches each of its neighboring lithium atoms [Fig. 1(b)], suffering a controlled collision [18] or an engineered interaction [16]. A fundamental difference with previous setups [17–19] is that the sublattice now moves as a whole, regardless of the internal states of the atoms. If the lattices are very deep and the atom-atom interaction is strong enough, this can be done with great precision.

To fix ideas, we will assume that the entangling operation between atoms in different sublattices is a CZ gate,  $U_{CZ} = \exp(-i\frac{\pi}{4}\sigma_{Cs}^z\sigma_{Li}^z)$ . After three parallel sets of operations, beginning with a product state  $(|0\rangle + |1\rangle)^{\otimes N}$ , we will arrive at a graph state

$$|G_{\circ}\rangle \sim \prod_{i \in A} \prod_{j \in \mathcal{N}(i)} U_{CZ}^{(i,j)} (|0\rangle + |1\rangle)^{\otimes N_A + N_B}, \quad (1)$$

where  $A$  and  $B$  denote the Cs and Li sublattices and  $\mathcal{N}(i) \subset B$  is the set of nearest neighbors to the potential well  $i$ . Note that, if instead of using the control phase one implements a control-NOT,  $U_{\text{CNOT}} = (1 + \sigma_{Li}^z) - (1 - \sigma_{Li}^z)\sigma_{Cs}^x$ , where the Cs absorbs the parity of its neighbors, we obtain what we call a “parity” multipartite entangled state

$$|P_{\circ}\rangle \sim \prod_{i \in A} \prod_{j \in \mathcal{N}(i)} U_{\text{CNOT}}^{(i,j)} (|0\rangle + |1\rangle)^{\otimes N_A + N_B}. \quad (2)$$

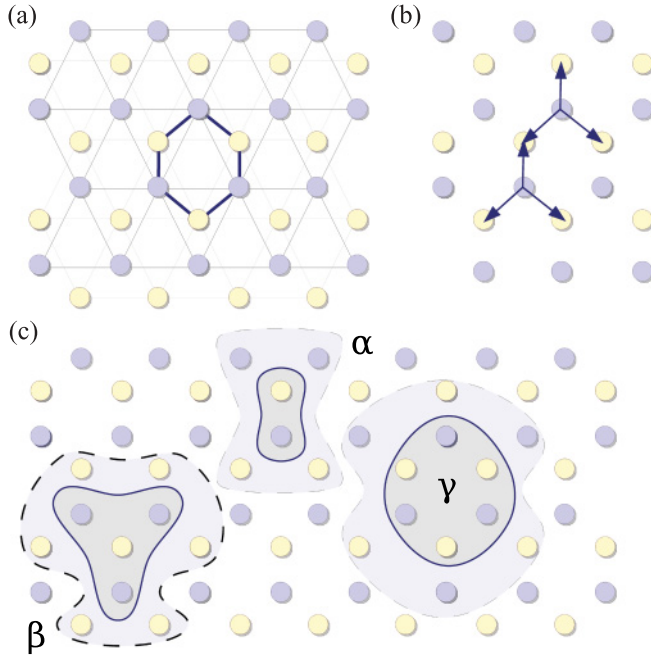


FIG. 1. (Color online) Bipartite lattice scheme. (a) We work with two species of atoms, Cs and Li, trapped in two independent triangular sublattices, which together form a honeycomb lattice. (b) A graph state can be generated by moving one of the sublattices along three different directions. (c) In this work we analyze the properties of localizable multipartite entanglement in small sets of 2 ( $\alpha$ ), 4 ( $\beta$ ), 6 ( $\gamma$ ), or more spins. Each of these regions  $\Omega$  is connected with its boundary  $\partial\Omega$  by two-qubit unitaries.

### III. ENTANGLEMENT WITNESSES

#### A. Global fidelity of graph states

All of the states that we can create by using the previous operations belong to the family of stabilizer states. In both cases we have a complete set of  $N_A + N_B$  local observables, the stabilizing operators  $g_i$ , that may take values  $\{-1, +1\}$ , and for which the states  $G_\circ$  and  $P_\circ$  are eigenstates with eigenvalue  $+1$  on all sites.<sup>1</sup> For instance, in the case of the graph state we have

$$g_i |G_\circ\rangle = +1 |G_\circ\rangle, \quad \forall i \in A \cup B \quad (3)$$

with the stabilizing operators  $g_i = \sigma_i^x \prod_{j \in \mathcal{N}(i)} \sigma_j^z$ . In general, given a set of lattice sites  $\Omega$ , we can construct a projector onto a stabilizer state containing those sites,

$$P_\Omega = \prod_{i \in \Omega} \frac{1}{2} (1 + g_i). \quad (4)$$

In theory we can use this projector to compute the fidelity of our experimentally realized state  $\rho$ , which is probably mixed, with respect to the objective  $G_\circ$  or  $P_\circ$ ,

$$F_{A \cup B} = \text{tr}(P_{A \cup B} \rho), \quad (5)$$

<sup>1</sup>The  $g_i$  operators are the generators of the so-called stabilizer group [21].

where the region under study now encloses the  $A$  and  $B$  sublattices. However, in practice this is already impossible for a few qubits, since the evaluation of  $F_\Omega$  requires us to measure  $2^{N_A + N_B}$  different observables coming from all possible products of the  $g_i$  operators. The difficulty of this task seems to be tantamount to performing a full tomography of the mixed state  $\rho$ .

#### B. Localizable fidelity

Instead of following this very complicated route, we will focus on two simpler questions, which are intimately related: (i) a notion of local fidelity to the stabilizer state and (ii) the existence and detection of genuine multipartite entanglement [22,23] in the lattice. In both cases we can extract a number, for example a fidelity or the expectation value of an entanglement witness,  $F(i)$  or  $W(i)$ , which is distributed over the 2D lattice of sites. With those numbers we can study the distribution of entanglement and how much our state has been affected by noise or decoherence.

Our notion of “localizable fidelity” builds on the fact that, given a simply connected set of sites  $\Omega$  and a perfect graph state  $|G_\circ\rangle$ , we can extract another perfect graph state in that region. One way to achieve this is by measuring the boundary qubits  $\partial\Omega$  [see Fig. 1(c)] and, depending on the outcome of those measurements, performing phase gates on the qubits that were immediately connected to them. An alternative but completely equivalent way is to disentangle the boundary with the same two-qubit unitaries we used to build the state,

$$\rho_\Omega = \text{tr} \left( \prod_{i \in \partial\Omega} \prod_{j \in \mathcal{N}(i)} U_{CZ}^{(i,j)} \rho_{A \cup B} \right). \quad (6)$$

The most important idea is that this procedure still can be applied if the initial state of the atomic ensemble is mixed,  $\rho_{A \cup B}$ , due to decoherence. In this case the fidelity of the final state is related to the same observable that we found before, that is

$$F_\Omega = \langle G_\Omega | \rho_\Omega | G_\Omega \rangle = \text{tr}(P_\Omega \rho_{A \cup B}), \quad (7)$$

and the fidelity of the final state only depends on how close  $\rho_{A \cup B}$  is to the eigenstates of the stabilizing operators that cover the region *and* the boundary,  $\Omega \cup \partial\Omega$ . The final observation is that the fidelity  $F_\Omega$  not only gives us local information about how close our state is to the graph state, but also is a witness for genuine multipartite entanglement in that region,  $W_\Omega = \frac{1}{2} \mathbb{1} - P_\Omega$  [24].

#### C. Optimized witnesses

However, even if  $\langle W \rangle < 0$  detects entanglement, the evaluation of this quantity seems to require a number of measurements that increases exponentially with the number of qubits. We thus need another ingredient, which is obtained by writing the fidelity as a product of two operators constructed from stabilizing operators corresponding to different sublattices,  $P_\Omega = P_{\Omega \cap A} P_{\Omega \cap B}$ , and by introducing a new operator [25]

$$\tilde{P}_\Omega = P_{\Omega \cap A} + P_{\Omega \cap B} - \mathbb{1} \leq P_\Omega. \quad (8)$$

This equation can be readily verified in the basis that diagonalizes both  $P_{\Omega \cap A}$  and  $P_{\Omega \cap B}$ , where the eigenvalues of the projectors can only be 0 or +1.

This observable provides a lower bound for the fidelity

$$F_{\Omega} \geq \langle \tilde{P}_{\Omega} \rangle, \quad (9)$$

and can be used to construct an entanglement witness

$$\tilde{W}_{\Omega} = \frac{1}{2} \mathbb{1} - \tilde{P}_{\Omega}. \quad (10)$$

The advantage is that now the quantities  $\langle P_{\Omega \cap A} \rangle$  and  $\langle P_{\Omega \cap B} \rangle$  can be extracted from just two settings of measurements. In particular, for the graph state one such expectation value

$$\langle P_{\Omega \cap A} \rangle = \left\langle \prod_{i \in \Omega \cap A} \frac{1}{2} \left( 1 + \sigma_i^x \prod_{j \in N(i)} \sigma_j^z \right) \right\rangle \quad (11)$$

is obtained by measuring  $\sigma^x$  in all Cs atoms ( $i \in \Omega \cap A$ ) and  $\sigma^z$  in the Li atoms [ $j \in N(i)$ ], while the other expectation value is obtained with the opposite measurement basis. Note also that, by postprocessing the *same* set of measurement results, we can compute the values  $\langle \tilde{P}_{\Omega} \rangle$  for any region  $\Omega$ , which allows us to produce two-dimensional displays of the distribution of localizable fidelity or the multipartite entanglement witness.

#### IV. SIMULATIONS

This section features a numerical simulation of a realization of our method in an experiment, taking possible practical sources of error into account. We have studied the degradation of the expectation value of the witness  $\tilde{W}_{\Omega}$  given in Eq. (10). In general it is not possible to compute the change of  $\langle P_{\Omega} \rangle$  easily, but we will take advantage of the facts that the witness is the sum of two functions of stabilizing operators corresponding to *different* sublattices and that for our sources of noise these expectation values have simple expressions, such as  $\langle P_{\Omega \cap A, B} \rangle = \prod_{i \in \Omega \cap A, B} (1 + \langle g_i \rangle) / 2$ , in which only the expectation values of isolated stabilizers appear,  $\langle g_i \rangle$ . As explained in the Appendix, we have considered various types

of noise [26] using the quantum channel formalism to compute the changes in  $\langle g_i \rangle$ :

(i) Dephasing, which is due to fluctuations in the energy levels of the atoms due to external fields,  $\epsilon_j(\rho) = \int d\theta_j \exp(-i\sigma^z \theta_j) \rho \exp(i\sigma^z \theta_j) p(\theta_j)$ . This map is repeated on all sites, with site-dependent uniformly distributed random phases in  $[-\epsilon_j, \epsilon_j]$ , degrading the stabilizing operator  $\langle g_i \rangle \rightarrow \langle g_i \rangle \prod_{i \in \Omega} \sin(2\epsilon_i) / 2\epsilon_i$ .

(ii) Imperfections in the gates that entangle pairs of sites,  $U_{CZ}^{(j,k)} \rightarrow U_{CZ}^{(j,k)} \exp(i\theta_{jk} \sigma_j^z \sigma_k^z)$ , where  $\theta_{jk}$  are again random variables, uniformly distributed in  $[-\epsilon_{jk}, \epsilon_{jk}]$ . This error introduces a factor in the expectation value of the stabilizing operators,  $\langle g_i \rangle \rightarrow \langle g_i \rangle \prod_{j \in N(i)} \frac{1}{2} [1 + \sin(2\epsilon_{ij}) / 2\epsilon_{ij}]$ , plus other terms that do not contribute to the witness (10).

(iii) Atom loss (AL), which introduces a new state in the lattice, the hole  $|h\rangle$ . In practice, it can be described by  $\epsilon_{AL}(\rho) = (1-p)\rho + p|0\rangle\langle 0|$ .

(iv) Spontaneous emission (SE),  $\epsilon_{SE}(\rho) = (1-p)\rho + p|0\rangle\langle 0|$ .

(v) The completely depolarizing (DP) channel,  $\epsilon_{DP}(\rho) = (1-p)\rho + \frac{p}{2}\mathbb{1}$ .

The last three sources of error have the same effect,  $\langle g_i \rangle \rightarrow (1-p)\langle g_i \rangle$ .

With these types of noise and decoherence, we studied the evolution of our witness operators and the overall description of a potential experiment that uses them. The results are shown in Figs. 2(a)–2(c), where we plot the values of  $\tilde{W}_{\alpha}$ ,  $\tilde{W}_{\beta}$ , and  $\tilde{W}_{\gamma}$ , interpolated using smooth functions that are centered and cover the affected regions,  $\alpha$ ,  $\beta$ , and  $\gamma$ , of two, four, and six qubits, respectively. The result is a two-dimensional map of the entanglement content, where the value of the witness is color coded either (a) on the link between two atoms,  $\alpha$ , (b) on the central atom and the star surrounding it,  $\beta$ , or (c) on the center of the six-atom plaquette,  $\gamma$ . In these particular plots we have combined all sources of decoherence, making some of them more relevant in different regions of the lattice. We have introduced a region of atoms subject to strong dephasing induced by a focused laser, covering the area marked by a circle. We have also emptied two sites, surrounded

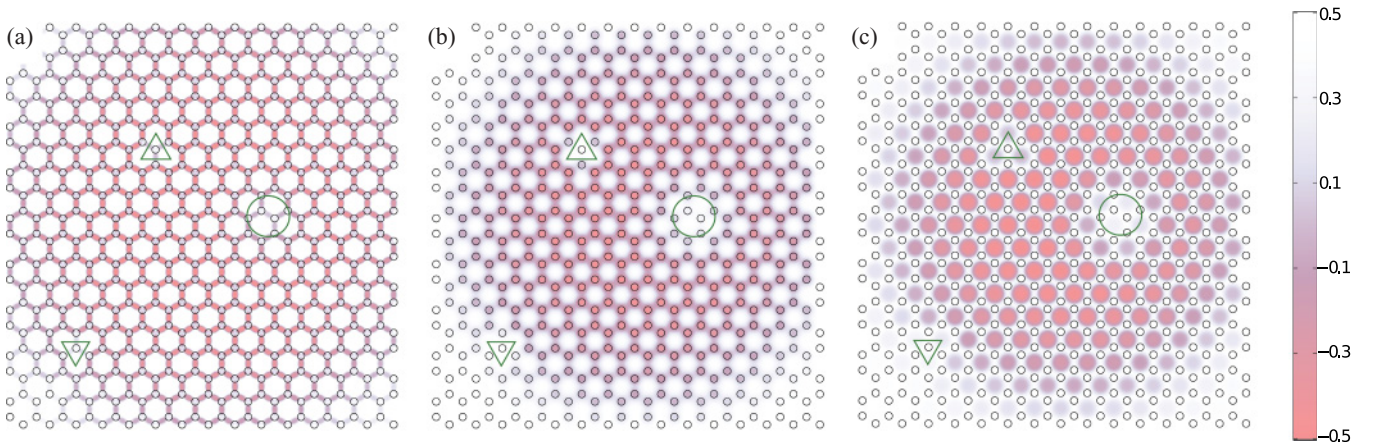


FIG. 2. (Color online) Two-dimensional distribution of the entanglement witnesses for (a) two, (b) four, and (c) six particle arrangements,  $\alpha$ ,  $\beta$ , and  $\gamma$  from Fig. 1(c), respectively. The value of the witness is color coded on the (a) links, (b) atoms, or (c) center of the plaquette. A negative value of the witness (red) denotes the existence of bi- or multipartite entanglement. All graphs present the same defects, consisting of two empty sites (triangles), atoms subject to strong dephasing (circle), and an increase of phase gate errors toward the edges of the trap.

by a triangle. These empty holes are numerically equivalent to having spontaneous emission with 100% probability. Finally, we have assumed that the phase gate is 100% accurate in the center of the lattice and acquires a 10% error at the boundary of the lattice.

We already appreciate interesting features in these simple simulations. The first one is that bipartite entanglement is less affected by noise than multiqubit arrangements. While we can reconstruct a Bell state close to the boundary with an 80% error, the four- and six-qubit states only have an appreciable value of the witness when the CZ gate is above 90% fidelity. The second feature is that the effect of local errors remains local. The sites, bonds, and plaquettes that share one or more qubits with the regions affected by atom loss or strong decoherence (circle and triangle in the plot) have positive values of the witness and do not have significant entanglement. However, one site or plaquette away from the region of influence of those defects, the witnesses recover their large negative value.

## V. CONCLUSIONS

In summary, we have presented a simple scheme for detecting bipartite and multipartite entanglement in two-dimensional lattices with ultracold atoms. The present study admits a straightforward generalization not only to other bipartite lattice setups, such as square lattices, but also to other interaction schemes ( $U_{\text{CNOT}}$ ), or to displacing each Cs atom not three, but one or two times. First of all, if the Cs atoms move along two directions, the result is an array of linear cluster states, with an entanglement witness that is a generalization of the previous ones, and that again relies only on two-measurement settings [24]. If instead we move each Cs atom only once, then the Cs-Li interact in pairs forming a macroscopic number of disconnected two-qubit singlets. In this case we do not need a witness but can rather compute the expectation value of the projector

$$P = \frac{1}{4} (\mathbb{1} + \sigma_{\text{Cs}}^x \sigma_{\text{Li}}^x + \sigma_{\text{Cs}}^y \sigma_{\text{Li}}^z + \sigma_{\text{Cs}}^z \sigma_{\text{Li}}^y), \quad (12)$$

using three experimental settings.

We must remark that our scheme only uses the facts that the lattice is bipartite and that it is possible to simultaneously measure the state of all lattice sites in each sublattice independently. In particular, while we have focused on a two-species setup [16,20], exactly the same protocols and measurement schemes can be used with the state-dependent optical lattices in previous experiments [18], combined with the new optics that allows imaging individual lattice sites [27]. The only difference is that, since we do not have different atoms on different sublattices, the measurement protocol has to be preceded by a global and local rotation of one sublattice to change its measurement basis. This is not too complicated and can be done by using two counterpropagating laser beams in an optical lattice configuration, such that their maxima of intensity coincide with just one sublattice.

Our proposal represents one of the first experimentally realizable schemes for mapping out the entanglement distribution and fidelity of a very large many-body correlated state. It also opens the path for the experimental detection of very large cluster states, a task which so far was not achievable using ultracold atoms in optical lattices, but which

becomes possible for ongoing experiments using two species of atoms and holographically generated trapping potentials [16]. In particular, we want to remark that the family of graph states in honeycomb lattices is a universal resource for measurement-based quantum computation, and that our scheme can be used to isolate regions of high fidelity in such resources.

## ACKNOWLEDGMENTS

G.T. acknowledges the support of the Spanish MICINN (Consolider-Ingenio 2010 project ‘‘QOIT,’’ Project No. FIS2009-12773-C02-02), the Basque Government (Project No. IT4720-10), and the ERC Starting Grant GEDEN-TQOPT. E.A. and J.J.G.R. acknowledge support from the Spanish MICINN Project No. FIS2009-10061, CSIC Project Ref. 200850I044, and the CAM project QUITMAD. E.A. acknowledges support from MEC Grant No. FPU2009-1761.

## APPENDIX: POSITIVE MAPS AND NOISE SOURCES

Any physical operation on a quantum state must be a trace-preserving positive map, which maps density matrices into density matrices. Furthermore, such operators admit a unique decomposition using a set of operators

$$\varepsilon(\rho) = \sum_k A_k \rho A_k^\dagger,$$

with the property  $\varepsilon(\mathbb{1}) = \mathbb{1}$ .

This description admits a generalization to expectation values. In other words, we also have a positive map description in the Heisenberg picture, where operators and observables, and not states, are changed. Using the definition  $\langle \Theta \rangle = \text{tr}(\Theta \rho)$ , the change in the expectation value can be expressed as

$$\langle \Theta \rangle_{\varepsilon(\rho)} = \text{tr} \left( \Theta \sum_k A_k \rho A_k^\dagger \right) = \langle \tilde{\varepsilon}(\Theta) \rangle,$$

where  $\tilde{\varepsilon}(\Theta) = \sum_k A_k^\dagger \Theta A_k$ .

We now want to estimate the effect of different positive maps on our entanglement witnesses. We will first focus on local error sources. It is important to observe that the expected values we want to calculate are of the general form

$$P = f(\sigma_{i \in A}^\alpha, \sigma_{i \in B}^\beta), \quad \alpha, \beta \in \{x, z\},$$

that is, they are functions of the same observables on each sublattice. This means that under local error sources the following relation applies:

$$P' = f(\tilde{\varepsilon}(\sigma_{i \in A}^\alpha), \tilde{\varepsilon}(\sigma_{i \in B}^\beta)).$$

Therefore, it suffices to compute how the operators change under the different local error sources. In each case, the decoherence channel will change the effective value of the stabilizer expectation value.

### 1. Dephasing

In this noise source, we have an average over random phases

$$\tilde{\varepsilon}(\sigma^x) = \int e^{-i\phi\sigma^z} \sigma^x e^{i\phi\sigma^z} p(\phi) d\phi.$$

If the distribution  $p(\phi)$  is symmetric, then

$$\tilde{\epsilon}(\sigma^x) = \int [\cos(2\phi) + i \sin(2\phi)\sigma^z] \sigma^x p(\phi) d\phi = (1 - \epsilon_i)\sigma^x,$$

with some error factor  $\epsilon_i$ . Since the  $\sigma^z$  operators are not affected, it is legitimate to say that the map induces a global change in the expected value  $g_i \rightarrow (1 - \epsilon_i)g_i$ .

## 2. Particle loss

This positive map has the form

$$\epsilon(\rho) = (1 - p)\rho + p|0\rangle\langle 0|,$$

which we can also write in Kraus form using the operators

$$A_0 = (1 - p)\mathbb{1}, \quad A_1 = p|0\rangle\langle 0|, \quad A_2 = p|0\rangle\langle 1|.$$

This means that the operators transform as

$$\tilde{\epsilon}(\Theta) = (1 - p)\Theta + p|0\rangle\langle 0|\Theta|0\rangle\langle 0|.$$

Thus the stabilizer operators are modified as

$$g_i \rightarrow (1 - p)^N \sigma_i^x \prod_{j \in N(i)} \sigma_j^z + g_i^\perp,$$

where  $N$  is the number of qubits in the stabilizer operator (4 in our case for the honeycomb lattice) and the  $g_i^\perp$  contain terms

that are going to vanish because they can be written in the form  $g_i \sigma_i^x \prod_{j \in N'(i)} \sigma_j^z$  or  $g_i \prod_{j \in N'(i)} \sigma_j^z$  with  $N'(i) \subseteq N(i)$ , so that their expectation values are zero.

## 3. Errors in the gates

We can proceed similarly, although some subtleties are to be taken into account. First of all we realize that instead of transforming the state, we can transform the stabilizer operators that appear in the expectation value

$$g_j \rightarrow e^{-i \sum_{k \in N(j)} \epsilon_{jk} \sigma_j^x \sigma_k^z} g_j e^{+i \sum_{k \in N(j)} \epsilon_{jk} \sigma_j^x \sigma_k^z}.$$

It can be seen that this is equivalent to performing the same transformation only on the  $\sigma_j^x$  operator

$$\sigma_j^x \rightarrow \prod_k [\cos(2\epsilon_{jk}) + i \sin(2\epsilon_{jk}) \sigma_j^x \sigma_k^z] \sigma_j^x.$$

Note that since we only have  $\sigma^x$  operators in one sublattice and  $\sigma^z$  on the other, the phases that we have here are uncorrelated among different  $\sigma^x$  operators. Furthermore, any term that contains a  $\sigma^z$  operator vanishes once we take expectation values, which means that we can replace  $\sigma_j^x \rightarrow (1 - \epsilon_j)\sigma_j^x$ , where  $\epsilon_j = \prod_k \int \epsilon_{jk} p_{jk}(\epsilon_{jk}) d\epsilon_{jk}$ . This shows that the outcome is a global reduction of the stabilizer expectation value.

- 
- [1] J. Pan, D. Bouwmeester, M. Daniell, H. Weinfurter, and A. Zeilinger, *Nature (London)* **403**, 515 (2000).
- [2] M. Bourennane, M. Eibl, C. Kurtsiefer, S. Gaertner, H. Weinfurter, O. Gühne, P. Hyllus, D. Bruß, M. Lewenstein, and A. Sanpera, *Phys. Rev. Lett.* **92**, 087902 (2004).
- [3] P. Walther, K. J. Resch, T. Rudolph, E. Schenck, H. Weinfurter, V. Vedral, M. Aspelmeyer, and A. Zeilinger, *Nature (London)* **434**, 169 (2005).
- [4] C. Lu, X. Zhou, O. Gühne, W. Gao, J. Zhang, Z. Yuan, A. Goebel, T. Yang, and J. Pan, *Nat. Phys.* **3**, 91 (2007).
- [5] A. Widera, O. Mandel, M. Greiner, S. Kreim, T. W. Hänsch, and I. Bloch, *Phys. Rev. Lett.* **92**, 160406 (2004).
- [6] M. Anderlini, P. J. Lee, B. L. Brown, J. Sebby-Strabley, W. D. Phillips, and J. V. Porto, *Nature (London)* **448**, 452 (2007).
- [7] H. Häffner *et al.*, *Nature (London)* **438**, 643 (2005).
- [8] D. Leibfried *et al.*, *Nature (London)* **438**, 639 (2005).
- [9] B. Julsgaard, A. Kozhekin, and E. S. Polzik, *Nature (London)* **413**, 400 (2001).
- [10] M. Horodecki, P. Horodecki, and R. Horodecki, *Phys. Lett. A* **223**, 1 (1996).
- [11] B. Terhal, *Phys. Lett. A* **271**, 319 (2000).
- [12] M. Lewenstein, B. Kraus, J. I. Cirac, and P. Horodecki, *Phys. Rev. A* **62**, 052310 (2000).
- [13] J. Cirac, P. Horodecki, F. Hulpke, B. Kraus, M. Lewenstein, A. Sanpera, and D. Bruß, *J. Mod. Opt.* **49**, 1399 (2002).
- [14] O. Gühne, P. Hyllus, D. Bruß, A. Ekert, M. Lewenstein, C. Macchiavello, and A. Sanpera, *Phys. Rev. A* **66**, 062305 (2002).
- [15] W. S. Bakr, J. I. Gillen, A. Peng, S. Fölling, and M. Greiner, *Nature (London)* **462**, 74 (2009).
- [16] K.-A. B. Soderberg, N. Gemelke, and C. Chin, *New J. Phys.* **11**, 055022 (2009).
- [17] H. J. Briegel and R. Raussendorf, *Phys. Rev. Lett.* **86**, 910 (2001).
- [18] O. Mandel, M. Greiner, A. Widera, T. Rom, T. W. Hänsch, and I. Bloch, *Nature (London)* **425**, 937 (2003).
- [19] D. Jaksch, H.-J. Briegel, J. I. Cirac, C. W. Gardiner, and P. Zoller, *Phys. Rev. Lett.* **82**, 1975 (1999).
- [20] A. Klinger, S. Degenkolb, N. Gemelke, K. Brickman Soderberg, and C. Chin, *Rev. Sci. Instrum.* **81**, 013109 (2010).
- [21] D. Gottesman, *Phys. Rev. A* **57**, 127 (1998).
- [22] C. A. Sackett *et al.*, *Nature (London)* **404**, 256 (2000).
- [23] A. Acín, D. Bruß, M. Lewenstein, and A. Sanpera, *Phys. Rev. Lett.* **87**, 040401 (2001).
- [24] G. Tóth and O. Gühne, *Phys. Rev. Lett.* **94**, 060501 (2005).
- [25] G. Tóth and O. Gühne, *Phys. Rev. A* **72**, 022340 (2005).
- [26] G. Benenti, G. Csati, and G. Strini, *Principles of Quantum Computation and Information* (World Scientific, Singapore, 2007), Volume II: Basic Tools and Special Topics.
- [27] W. S. Bakr, J. I. Gillen, A. Peng, S. Fölling, and M. Greiner, *Nature (London)* **462**, 74 (2009).